



# Femtoscopia reveals how (anti-)deuteron is formed at the LHC

Kai-Jia Sun<sup>1,2</sup>

Received: 12 December 2025 / Revised: 13 December 2025 / Accepted: 13 December 2025 / Published online: 29 January 2026

© The Author(s), under exclusive licence to China Science Publishing & Media Ltd. (Science Press), Shanghai Institute of Applied Physics, the Chinese Academy of Sciences, Chinese Nuclear Society 2026

The production of light (anti-)nuclei in high-energy collisions has long posed an apparent paradox: How can loosely bound systems such as the anti-deuteron with a binding energy of only 2.23 MeV be formed and survive in the extreme hot and dense hadronic environment emerging from proton–proton (pp) and heavy-ion collisions, where characteristic thermal energies exceed 100 MeV? A new femtoscopy analysis published on *Nature* [1] by the ALICE Collaboration at the Large Hadron Collider (LHC) delivers the clearest answer to date. By measuring pion-(anti-)deuteron momentum correlations in high-multiplicity pp collisions at  $\sqrt{s} = 13$  TeV, the experiment demonstrated that most (anti-)deuterons are not produced directly at hadronization, but instead originating from meson-catalyzed reactions [2] following the decay of short-lived baryonic resonances, most notably the  $\Delta(1232)$ . This result provides long-sought microscopic insight into how fragile (anti-)nuclei emerge in ultra-relativistic hadronic environments, from collider events to cosmic rays.

Light nuclei and antinuclei, such as deuterons (d), tritons ( ${}^3\text{H}$ ), helium-3 ( ${}^3\text{He}$ ), helium-4 ( ${}^4\text{He}$ ), and their antiparticles, have been measured with increasing precision across collision systems and energies, from heavy-ion collisions to pp collisions [3–11]. This phenomenon, known as ‘little bang nucleosynthesis’ [2, 12] or ‘snowballs in hell’ [13, 14], connects directly to fundamental questions about matter–antimatter symmetry [15], phase transitions in quantum chromodynamics (QCD) [16, 17], and dark-matter searches [18, 19].

While their integrated yields are often described surprisingly well by the statistical hadronization model of

quark–gluon plasma [20], their microscopic formation remains far from settled [21–24]. The deuteron’s binding energy is two orders of magnitude smaller than the temperature of hadronic matter produced in pp or Pb+Pb collisions. In such an environment, ‘direct’ emission from the hadronization of quark–gluon plasma or the chemical freeze-out hypersurface appears implausible, and any loosely bound system produced early would almost certainly be destroyed by subsequent hadronic rescatterings. Final-state coalescence models offer a different scenario in which nucleons close in phase space can merge into bound states at the very late kinetic freeze-out [25–28]. In the microscopic transport approach, it has been shown that pion-catalyzed reactions (e.g.  $\pi\text{NN} \leftrightarrow \pi\text{d}$ ,  $\pi\text{Nd} \leftrightarrow \pi{}^3\text{He}$ ) do not significantly change the deuteron production in central Pb+Pb and Au+Au collisions [29], but reduce the triton and Helium-3 yield by approximately a factor of 1.8 [2]. For the forward pion-catalyzed reaction  $\pi\text{NN} \rightarrow \pi\text{d}$ , it can be viewed as a two-step process of  $\pi\text{N} \rightarrow \Delta$  and  $\Delta\text{N} \rightarrow \pi\text{d}$ , and a deuteron is produced via nucleon fusion following a  $\Delta \rightarrow \pi\text{N}$  decay. The decayed pion is kinematically correlated with the nucleon that subsequently participates in forming the deuteron. This correlation manifests as a distinct  $\Delta$  resonant structure in the pion-deuteron correlation function in momentum space, as the reaction rate reaches maximum at relative momenta reflecting the  $\Delta$  mass and decay kinematics [2].

The ALICE measurement exploits this signature through pion-deuteron ( $\pi$ -d) femtoscopy [1]. Femtoscopy analyzes momentum correlations at relative distances down to order of 1 fm ( $10^{-15}$  m) [30–33] and has become a precision tool for studying strong interactions [34–37] and exotic hadrons [38]. The new ALICE data reveal a pronounced resonance peak associated with  $\Delta$  decay, providing direct evidence that (anti-)deuterons form predominantly through resonance-fed secondary processes.

The key experimental observable is the momentum correlation function,

✉ Kai-Jia Sun  
kjsun@fudan.edu.cn

<sup>1</sup> Shanghai Research Center for Theoretical Nuclear Physics, NSFC and Fudan University, Shanghai 200438, China

<sup>2</sup> Key Laboratory of Nuclear Physics and Ion-Beam Application (MOE), Institute of Modern Physics, Fudan University, Shanghai 200433, China

$$C(k^*) = \mathcal{N} \frac{N_{\text{same}}(k^*)}{N_{\text{mixed}}(k^*)}, \quad (1)$$

where  $k^*$  is the momentum of either particle in the pair rest frame.  $N_{\text{same}}(k^*)$  denotes the distribution of relative momenta for particle pairs from the same event, while  $N_{\text{mixed}}(k^*)$  provides an uncorrelated reference constructed by combining particles from different events. The factor  $\mathcal{N}$  normalizes the correlation function so that  $C(k^*)$  approaches unity at large  $k^*$ .

Intriguing correlations can arise from final-state strong and Coulomb interactions [39, 40], quantum statistics [39], or resonance decays [40]. In general, attractive interactions enhance  $C(k^*)$  at low  $k^*$ , whereas repulsive interactions suppress it.

ALICE measures  $\pi^-d$  and  $\pi^- \bar{d}$  correlations in high-multiplicity  $pp$  collisions at  $\sqrt{s} = 13$  TeV with excellent particle identification, achieving purities of 99–100%. The correlation functions shown in Fig. 1 exhibit a prominent peak associated with  $\Delta$  resonance decay. The data are then modeled using

$$C_{\text{fit}}(k^*) = \epsilon(k^*) \otimes B(k^*) [\lambda_{\text{gen}} C_{\text{gen}}(k^*) + (1 - \lambda_{\text{gen}})], \quad (2)$$

where  $\epsilon(k^*)$  accounts for momentum resolution,  $B(k^*)$  for residual backgrounds, and  $\lambda_{\text{gen}}$  for the fraction of genuine pairs. The genuine correlation function  $C_{\text{gen}}(k^*)$  includes Coulomb and strong interactions plus the  $\Delta$  contribution and is computed via CATS [41] assuming an effective source radius  $r_{\text{eff}} = 1.51 \pm 0.12$  fm.

Final-state Coulomb and strong interactions generate a monotonic enhancement (suppression) for  $\pi^-d$  ( $\pi^+d$ ) pairs at low relative momentum ( $k^* < 50$  MeV/ $c$ ), while the  $\Delta$  resonance produces strong peaks around  $k^* \approx 150$  MeV/ $c$  in both correlation functions.

By integrating the  $\Delta$  peak, ALICE finds that  $60.6 \pm 4.1\%$  of detected deuterons contain a nucleon produced in a  $\Delta$  decay. Accounting for all short-lived resonances yields a total resonance-fed fraction of  $88.9 \pm 6.3\%$ . Thus, meson-catalyzed fusion with resonance-decay nucleons dominates (anti-)deuteron formation at the LHC.

This conclusion is reinforced by a recent theoretical study [42] that reproduces the observed resonant structure in both pion-proton ( $\pi$ -p) and pion-deuteron ( $\pi$ -d) correlation functions by solving relativistic kinetic equations for  $\pi NN \leftrightarrow \pi d$  on an event-by-event basis. The model–data comparison further indicates a strong downward in-medium shift of the  $\Delta(1232)$  mass by approximately 70 MeV/ $c^2$  [1]. Such a reduction from  $m_{\Delta} = 1.232$  GeV/ $c^2$  to 1.162 GeV/ $c^2$  may reflect strong in-medium modifications, possibly linked to partial chiral-symmetry restoration [43]. Traditional coalescence models reproduce only about half of the observed peak, and statistical hadronization fails to

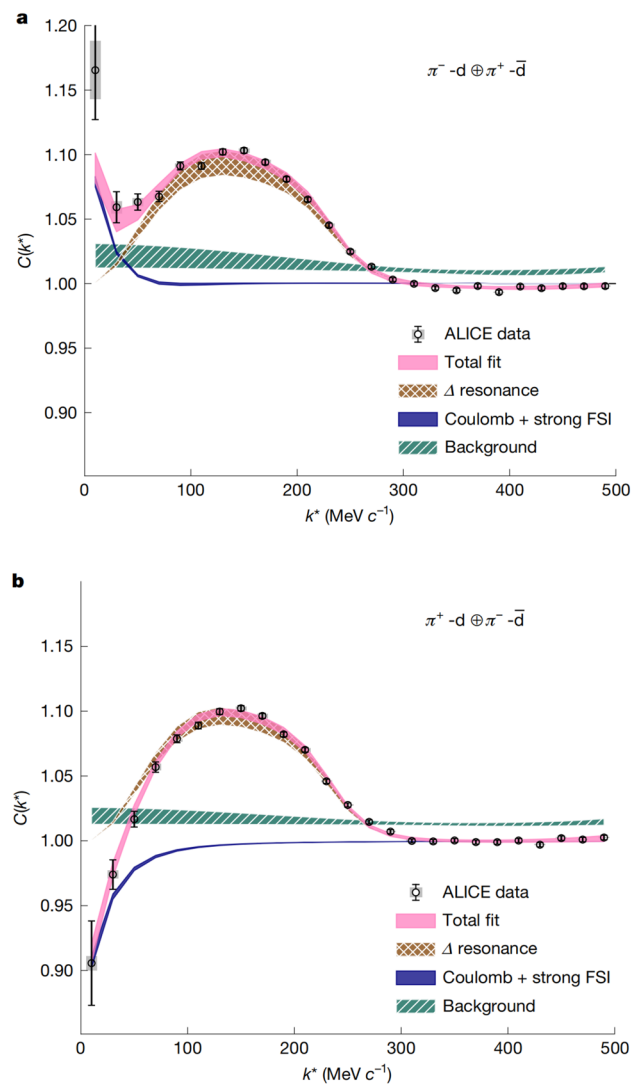


**Fig. 1** (Color online) Measured  $\pi^-d$  (upper panel) and  $\pi^+d$  (lower panel) correlation functions compared with model fits. The brown cross-hatched bands show the contributions from the  $\Delta$  resonance, the blue bands the Coulomb interaction, and the teal diagonally hatched bands the residual background. The magenta bands represent the total fit. Figure taken from Ref. [1]

generate any resonance structure, highlighting the unique discriminatory power of pion-nucleus femtoscopy for unraveling (anti-)nuclei production mechanisms.

In summary, ALICE has uncovered the dominant mechanism of (anti-)deuteron formation at the LHC using the novel technique of pion-nucleus correlation femtoscopy. The measurement provides the first compelling evidence that most (anti-)deuterons originate from resonance decays followed by pion-catalyzed fusion rather than direct emission. This finding resolves a long-standing puzzle in light-nucleus production and establishes a clear microscopic pathway for (anti-)nucleosynthesis in high-energy collisions.

A complete understanding of these results calls for further studies on the in-medium properties of light nuclei and advances in relativistic kinetic theory that incorporate multi-body correlations and off-shell quantum effects at high temperatures [44, 45]. Extending femtoscopy measurements to heavier (hyper-)nuclei will open new opportunities to probe their formation mechanisms and may even help constrain the production of exotic hadronic states [38, 46–48] in hot and dense matter.

**Acknowledgements** This work was supported in part by the National Key Research and Development Project of China (No. 2024YFA1612500), the National Natural Science Foundation of China (Nos. 12422509, 12375121, and 12547102).

## References

1. S. Acharya, A. Agarwal, G. Aglieri Rinella et al., Observation of deuteron and antideuteron formation from resonance-decay nucleons. *Nature* **648**, 306–311 (2025). <https://doi.org/10.1038/s41586-025-09775-5>
2. K.J. Sun, R. Wang, C.M. Ko et al., Unveiling the dynamics of little-bang nucleosynthesis. *Nat. Commun.* **15**, 1074 (2024). <https://doi.org/10.1038/s41467-024-45474-x>
3. B.I. Abelev, M. Aggarwal, Z. Ahammed et al., Observation of an antimatter hypernucleus. *Science* **328**, 58–62 (2010). <https://doi.org/10.1126/science.1183980>
4. H. Agakishiev, M. Aggarwal, Z. Ahammed, et al., Observation of the antimatter helium-4 nucleus. *Nature* **473**, 353 (2011). [Erratum: *Nature* 475, 412 (2011)]. <https://doi.org/10.1038/nature10079>
5. M. Abdallah, B. Aboona, J. Adam et al., Measurements of  ${}^3_{\Lambda}\text{H}$  and  ${}^4_{\Lambda}\text{H}$  lifetimes and yields in Au+Au collisions in the high Baryon density region. *Phys. Rev. Lett.* **128**, 202301 (2022). <https://doi.org/10.1103/PhysRevLett.128.202301>
6. S. Acharya, D. Adamová, A. Adler et al., Hypertriton production in p-Pb collisions at  $\sqrt{s_{\text{NN}}}=5.02$  TeV. *Phys. Rev. Lett.* **128**, 252003 (2022). <https://doi.org/10.1103/PhysRevLett.128.252003>
7. S. Acharya, D. Adamová, A. Adler et al., Measurement of the low-energy antideuteron inelastic cross section. *Phys. Rev. Lett.* **125**, 162001 (2020). <https://doi.org/10.1103/PhysRevLett.125.162001>
8. S. Acharya, D. Adamová, A. Adler et al., Enhanced deuteron coalescence probability in jets. *Phys. Rev. Lett.* **131**, 042301 (2023). <https://doi.org/10.1103/PhysRevLett.131.042301>
9. M. Abdulhamid, B. Aboona, J. Adam et al., Observation of the antimatter hypernucleus  ${}^4_{\Lambda}\bar{H}$ . *Nature* **632**, 1026–1031 (2024). <https://doi.org/10.1038/s41586-024-07823-0>
10. S. Acharya, A. Agarwal, G. Aglieri Rinella et al., First measurement of  $A = 4$  hypernuclei and antihypernuclei at the LHC. *Phys. Rev. Lett.* **134**, 162301 (2025). <https://doi.org/10.1103/PhysRevLett.134.162301>
11. T. Shao, J. Chen, J. Pochodzalla et al., Measurement of  ${}^6\text{H}$  ground state energy in an electron scattering experiment at MAMI-A1. *Phys. Rev. Lett.* **134**, 162501 (2025). <https://doi.org/10.1103/PhysRevLett.134.162501>
12. M. Bleicher, Nucleosynthesis in the little bang. *Nucl. Sci. Tech.* **35**, 129 (2024). <https://doi.org/10.1007/s41365-024-01477-3>
13. P. Braun-Münzinger, B. Dönigus, N. Löhner, ALICE investigates ‘snowballs in hell’. *CERN Courier* 55. <https://cerncourier.com/a/alice-investigates-snowballs-in-hell/>
14. E. Braaten, K. Ingles, J. Pickett, Explaining snowball-in-hell phenomena in heavy-ion collisions using a novel thermodynamic variable. *Phys. Rev. Lett.* **134**, 252301 (2025). <https://doi.org/10.1103/7cjr-fgdw>
15. ALICE Collaboration, Precision measurement of the mass difference between light nuclei and anti-nuclei. *Nature Phys.* **11**, 811–814 (2015). <https://doi.org/10.1038/nphys3432>
16. K.J. Sun, L.W. Chen, C.M. Ko et al., Probing QCD critical fluctuations from light nuclei production in relativistic heavy-ion collisions. *Phys. Lett. B* **774**, 103–107 (2017). <https://doi.org/10.1016/j.physletb.2017.09.056>
17. M. Abdulhamid, B. Aboona, J. Adam et al., Beam energy dependence of triton production and yield ratio ( $N_t \times N_p / N_d^2$ ) in Au+Au collisions at RHIC. *Phys. Rev. Lett.* **130**, 202301 (2023). <https://doi.org/10.1103/PhysRevLett.130.202301>
18. P. von Doetinchem, K. Perez, T. Aramaki et al., Cosmic-ray anti-nuclei as messengers of new physics: status and outlook for the new decade. *J. Cosmol. Astropart. Phys.* **08**, 035 (2020). <https://doi.org/10.1088/1475-7516/2020/08/035>
19. S. Acharya, D. Adamová, A. Adler et al., Measurement of anti- ${}^3\text{He}$  nuclei absorption in matter and impact on their propagation in the Galaxy. *Nat. Phys.* **19**, 61–71 (2023). <https://doi.org/10.1038/s41567-022-01804-8>
20. A. Andronic, P. Braun-Munzinger, K. Redlich et al., Decoding the phase structure of QCD via particle production at high energy. *Nature* **561**, 321–330 (2018). <https://doi.org/10.1038/s41586-018-0491-6>
21. S.T. Butler, C.A. Pearson, Deuterons from high-energy proton bombardment of matter. *Phys. Rev.* **129**, 836–842 (1963). <https://doi.org/10.1103/PhysRev.129.836>
22. L.P. Csernai, J.I. Kapusta, Entropy and cluster production in nuclear collisions. *Phys. Rep.* **131**, 223–318 (1986). [https://doi.org/10.1016/0370-1573\(86\)90031-1](https://doi.org/10.1016/0370-1573(86)90031-1)
23. P. Braun-Munzinger, B. Dönigus, Loosely-bound objects produced in nuclear collisions at the LHC. *Nucl. Phys. A* **987**, 144–201 (2019). <https://doi.org/10.1016/j.nuclphysa.2019.02.006>
24. J. Chen, D. Keane, Y.G. Ma et al., Antinuclei in heavy-ion collisions. *Phys. Rep.* **760**, 1–39 (2018). <https://doi.org/10.1016/j.physrep.2018.07.002>
25. R. Scheibl, U. Heinz, Coalescence and flow in ultrarelativistic heavy ion collisions. *Phys. Rev. C* **59**, 1585–1602 (1999). <https://doi.org/10.1103/PhysRevC.59.1585>
26. F. Bellini, K. Blum, A.P. Kalweit et al., Examination of coalescence as the origin of nuclei in hadronic collisions. *Phys. Rev. C* **103**, 014907 (2021). <https://doi.org/10.1103/PhysRevC.103.014907>
27. K.J. Sun, C.M. Ko, B. Dönigus, Suppression of light nuclei production in collisions of small systems at the Large Hadron Collider. *Phys. Lett. B* **792**, 132–137 (2019). <https://doi.org/10.1016/j.physletb.2019.03.033>
28. K.J. Sun, D.N. Liu, Y.P. Zheng et al., Deciphering hypertriton and antihypertriton spins from their global polarizations in heavy-ion collisions. *Phys. Rev. Lett.* **134**, 022301 (2025). <https://doi.org/10.1103/PhysRevLett.134.022301>
29. D. Oliinychenko, L.G. Pang, H. Elfner et al., Microscopic study of deuteron production in PbPb collisions at  $\sqrt{s} = 2.76$  TeV via hydrodynamics and a hadronic afterburner. *Phys. Rev. C* **99**, 044907 (2019). <https://doi.org/10.1103/PhysRevC.99.044907>
30. R. Hanbury Brown, R.Q. Twiss, A Test of a new type of stellar interferometer on Sirius. *Nature* **178**, 1046–1048 (1956). <https://doi.org/10.1038/1781046a0>
31. R. Lednicky, V.L. Lyuboshits, Final state interaction effect on pairing correlations between particles with small relative momenta. *Yad. Fiz.* **35**, 1316–1330 (1981)

32. U.W. Heinz, B.V. Jacak, Two particle correlations in relativistic heavy ion collisions. *Ann. Rev. Nucl. Part. Sci.* **49**, 529–579 (1999). <https://doi.org/10.1146/annurev.nucl.49.1.529>
33. M.A. Lisa, S. Pratt, R. Soltz et al., Femtoscopy in relativistic heavy ion collisions. *Ann. Rev. Nucl. Part. Sci.* **55**, 357–402 (2005). <https://doi.org/10.1146/annurev.nucl.55.090704.151533>
34. L. Adamczyk, J. Adkins, G. Agakishiev et al., Measurement of interaction between antiprotons. *Nature* **527**, 345–348 (2015). <https://doi.org/10.1038/nature15724>
35. A. Collaboration, et al., Unveiling the strong interaction among hadrons at the LHC. *Nature* **588**, 232–238 (2020). [Erratum: *Nature* 590, E13 (2021)]. <https://doi.org/10.1038/s41586-020-3001-6>
36. S. Acharya, D. Adamová, S.P. Adhya et al., Scattering studies with low-energy kaon-proton femtoscopy in proton-proton collisions at the LHC. *Phys. Rev. Lett.* **124**, 092301 (2020). <https://doi.org/10.1103/PhysRevLett.124.092301>
37. D. Si, S. Xiao, Z. Qin et al., Extracting neutron-neutron interaction strength and spatiotemporal dynamics of neutron emission from the two-particle correlation function. *Phys. Rev. Lett.* **134**, 222301 (2025). <https://doi.org/10.1103/PhysRevLett.134.222301>
38. M.Z. Liu, Y.W. Pan, Z.W. Liu et al., Three ways to decipher the nature of exotic hadrons: multiplets, three-body hadronic molecules, and correlation functions. *Phys. Rep.* **1108**, 1–108 (2025). <https://doi.org/10.1016/j.physrep.2024.12.001>
39. S.E. Koonin, Proton pictures of high-energy nuclear collisions. *Phys. Lett. B* **70**, 43–47 (1977). [https://doi.org/10.1016/0370-2693\(77\)90340-9](https://doi.org/10.1016/0370-2693(77)90340-9)
40. U.A. Wiedemann, U.W. Heinz, Resonance contributions to HBT correlation radii. *Phys. Rev. C* **56**, 3265–3286 (1997). <https://doi.org/10.1103/PhysRevC.56.3265>
41. D.L. Mihaylov, V. Mantovani Sarti, O.W. Arnold et al., A femtosopic correlation analysis tool using the Schrödinger equation (CATS). *Eur. Phys. J. C* **78**, 394 (2018). <https://doi.org/10.1140/epjc/s10052-018-5859-0>
42. L.Y. Zhang, C.M. Ko, Y.G. Ma, et al., Shedding light on (anti-) nuclei production with pion-nucleus femtoscopy. [arXiv:2511.10298](https://arxiv.org/abs/2511.10298)
43. J.M. Torres-Rincon, B. Sintès, J. Aichelin, Flavor dependence of baryon melting temperature in effective models of QCD. *Phys. Rev. C* **91**, 065206 (2015). <https://doi.org/10.1103/PhysRevC.91.065206>
44. R. Wang, Y.G. Ma, L.W. Chen et al., Kinetic approach of light-nuclei production in intermediate-energy heavy-ion collisions. *Phys. Rev. C* **108**, L031601 (2023). <https://doi.org/10.1103/PhysRevC.108.L031601>
45. Z. Tang, B. Wu, A. Hanlon et al., Quarkonium spectroscopy in the quark-gluon plasma. *Phys. Rev. Lett.* **135**, 142302 (2025). <https://doi.org/10.1103/PhysRevLett.135.142302>
46. F.K. Guo, C. Hanhart, U.G. Meißner, et al., Hadronic molecules. *Rev. Mod. Phys.* **90**, 015004 (2018). [Erratum: *Rev. Mod. Phys.* **94**, 029901 (2022)]. <https://doi.org/10.1103/RevModPhys.90.015004>
47. J.H. Chen, J. Chen, F.K. Guo et al., Production of exotic hadrons in pp and nuclear collisions. *Nucl. Sci. Tech.* **36**, 55 (2025). <https://doi.org/10.1007/s41365-025-01664-w>
48. Z.W. Liu, J.M. Xie, J.X. Lu, et al., Probing the di- $J/\Psi$  interaction and the nature of  $X(6200)$  with femtosopic correlation functions. [arXiv:2512.10459](https://arxiv.org/abs/2512.10459)